




Original Article

# Laboratory Reconstructions of Bicycle Helmet Damage: Investigation of Cyclist Head Impacts Using Oblique Impacts and Computed Tomography

MEGAN L. BLAND <sup>1</sup>, CRAIG McNALLY,<sup>1</sup> JESSICA B. CICCHINO,<sup>2</sup>  
DAVID S. ZUBY,<sup>2</sup> BECKY C. MUELLER,<sup>2</sup> MELISSA L. MCCARTHY,<sup>3</sup>  
CRAIG D. NEWGARD,<sup>4</sup> PAIGE E. KULIE,<sup>5</sup> BRITTANY N. ARNOLD,<sup>4</sup>  
and STEVEN ROWSON<sup>1</sup>

<sup>1</sup>Department of Biomedical Engineering and Mechanics, Virginia Tech, 343 Kelly Hall, 325 Stanger Street, Blacksburg, VA 24061, USA; <sup>2</sup>Insurance Institute for Highway Safety, 988 Dairy Road, Ruckersville, VA 22968, USA; <sup>3</sup>George Washington University Milken Institute School of Public Health, 950 New Hampshire Avenue NW, Washington, DC 20052, USA;

<sup>4</sup>Department of Emergency Medicine, Center for Policy and Research in Emergency Medicine, Oregon Health & Science University, 3181 SW Jackson Park Road, CR-114, Portland, OR 97239, USA; and <sup>5</sup>Department of Emergency Medicine, George Washington University Medical Center, 2120 L Street NW, Suite 450, Washington, DC 20037, USA

(Received 19 June 2020; accepted 11 September 2020; published online 24 September 2020)

Associate Editor Joel D Stitzel oversaw the review of this article.

**Abstract**—Although head injuries are common in cycling, exact conditions associated with cyclist head impacts are difficult to determine. Previous studies have attempted to reverse engineer cyclist head impacts by reconstructing bicycle helmet residual damage, but they have been limited by simplified damage assessment and testing. The present study seeks to enhance knowledge of cyclist head impact conditions by reconstructing helmet damage using advanced impact testing and damage quantification techniques. Damage to 18 helmets from cyclists treated in emergency departments was quantified using computed tomography and reconstructed using oblique impacts. Damage metrics were related to normal and tangential velocities from impact tests as well as peak linear accelerations (PLA) and peak rotational velocities (PRV) using case-specific regression models. Models then allowed original impact conditions and kinematics to be estimated for each case. Helmets were most frequently damaged at the front and sides, often near the rim. Concussion was the most common, non-superficial head injury. Normal velocity and PLA distributions were similar to previous studies, with median values of 3.4 m/s and 102.5 g. Associated tangential velocity and PRV medians were 3.8 m/s and 22.3 rad/s. Results can inform future oblique impact testing conditions, enabling improved helmet evaluation and design.

**Keywords**—Head injury, Concussion, Biomechanics, Oblique impact, Accident reconstruction.

## INTRODUCTION

Cycling is becoming increasingly popular in the United States, with over 103 million Americans reported to having ridden a bicycle in 2015 (total population approximately 322 million in 2015).<sup>1</sup> However, its growing popularity is paralleled by increases in related injuries. Cycling-related hospital admissions have grown 120% in 15 years,<sup>31</sup> and in 2015 there was a 12% increase in fatalities over the previous year.<sup>1</sup> Head injuries are among the most common and serious of injuries from these accidents.<sup>11,33</sup> Bicycle helmets, which have been shown to reduce risk of head injury,<sup>26,33</sup> are presently designed around impact tests prescribed in safety standards. Standards testing requires that helmets be fitted onto a surrogate headform and subjected to guided drop tests. The helmeted headform impacts an anvil from an angle normal to the anvil surface (termed “normal” impact herein), and the headform peak linear acceleration (PLA) must stay below a set threshold for the helmet to pass. In the US Consumer Product Safety Com-

Address correspondence to Megan L. Bland, Department of Biomedical Engineering and Mechanics, Virginia Tech, 343 Kelly Hall, 325 Stanger Street, Blacksburg, VA 24061, USA. Electronic mail: mbland27@vt.edu

mission (CPSC) standard, this threshold is 300 g ( $> 50\%$  risk of skull fracture or severe brain injury<sup>22</sup>).<sup>12</sup>

While standards ensure a minimal adequate level of protection for bicycle helmets, research suggests that real-world cyclist head impacts are much more complex than standards' testing. Namely, cyclist head impacts typically occur oblique to the impact surface, comprising of normal and tangential incident velocities and producing both linear and rotational head impact kinematics.<sup>7,27</sup> Linear kinematics are linked to pressure gradients causing focal injury such as skull fracture or cerebral contusion, while rotational kinematics are highly correlated to brain tissue shear strain causing diffuse injury such as concussion or diffuse axonal injury.<sup>16,18–20</sup>

A number of oblique impact rigs have been developed to more holistically evaluate bicycle helmet performance.<sup>2,3,24,25</sup> Although this marks an improvement in helmet testing, head impact conditions common to cycling are still relatively unclear. Defining these conditions is challenging due to the unpredictability of cyclist crashes. Direct instrumentation of cyclists would provide optimal data; however, because cyclist crashes are involuntary events, head impacts are generally infrequent per rider, rendering collection of naturalistic data through instrumented cyclists impractical. Alternatively, instrumenting volunteers and instructing them to crash while cycling is unethical due to the considerable injury risks involved. Previous studies have thus approached the study of cyclist head impacts through computational simulations<sup>7,27</sup> or laboratory reconstructions of helmet damage from real-world accidents.<sup>32,34</sup>

Computational simulations of cyclist accidents use multibody and finite element models to estimate the conditions associated with cyclist head impacts.<sup>7,27</sup> Results from these studies provide invaluable insight into the nature of such impacts; however, these simulations are limited by a lack of real-world cyclist head impact data available for validation. Helmet damage reconstructions rely on the permanent crushing of conventional bicycle helmets' expanded polystyrene (EPS) liner that serves to dissipate energy during a head impact. The residual damage can be recreated using laboratory impact tests to undamaged samples of an identical helmet. Although this approach has potential, past reconstruction studies have been limited by simplified test setups and damage assessment techniques.<sup>32,34</sup> These studies have utilized normal impact testing, neglecting to simulate the oblique nature of cyclist head impacts, and have quantified damage through visual inspection of helmet liners. Aside from reduced precision associated with visual inspection, this approach requires removing the helmet shell from the liner to take measurements. Many manufacturers

now use in-molding to couple helmet liners to shells, increasing the potential for considerable liner damage to accrue during shell removal.

More advanced impact testing and damage quantification methods have been proposed for helmet damage reconstructions in recent years, largely in the motorcycle helmet space.<sup>5,8,21</sup> Main advances include the use of computed tomography (CT) to quantify liner damage non-destructively while also accounting for potential gaps between the liner and shell.<sup>5,21</sup> CT scans can be converted into 3D models of the liner, which can then be overlaid with an identical, undamaged liner model to compute damage metrics such as crush depth or volume. Previous work has demonstrated that CT-derived damage metrics can be recreated with high reliability and precision.<sup>5</sup>

Reconstructions could also be enhanced through oblique impact testing. One motorcycle helmet damage reconstruction study conducted oblique impacts using a number of anvil types and reported that helmet shell and liner damage was reflective of the angle and shape of the anvil surface.<sup>8</sup> To the authors' knowledge, no peer-reviewed study has employed oblique impact testing for bicycle helmet damage reconstruction, and very few have applied CT-based damage quantification to bicycle helmets. Use of these advanced approaches to reverse engineer conditions of cyclist head impacts could greatly enrich understanding of these impacts, which could in turn stimulate improved helmet design.

The objective of this study was to enhance understanding of cyclist head impacts by reconstructing real-world bicycle helmet damage using oblique impact testing and CT-based damage quantification.

## MATERIALS AND METHODS

### *Case Information and Exclusion Criteria*

Accident-damaged bicycle helmets were donated by cyclists who experienced crashes in an urban environment and were evaluated in the emergency department at George Washington University Hospital (Washington, D.C.), Oregon Health and Sciences University (Portland), Beth Israel Deaconess (Boston), or NYU Langone Medical Center (New York City) from 2015 to 2017. Cyclists were able to donate their helmet as part of an Insurance Institute for Highway Safety (IIHS) study investigating cycling infrastructure effectiveness.<sup>9</sup> This overarching study stipulated that participants be able to give informed consent and recall the route they were biking at the time of the accident (excluding cases involving severe memory loss). Cases involving fatalities or children were excluded, as were accidents involving trick or tandem riding. Donated

helmets were accompanied by associated medical reports, details of surrounding road characteristics, and the patient's description of the accident. Related protocols were approved by each hospital's Institutional Review Board (IRB) as well as the Virginia Tech IRB (17-1036).

Donated helmets and associated information were analyzed to determine the candidacy of each case for reconstruction. A total of 58 helmets were received. Helmets were immediately excluded if the patient claimed that their helmet was not damaged during the accident (5 cases). Cases involving facial fracture were also excluded (6 cases), as this implies that the impact force was primarily directed at the face rather than the helmet. Helmet damage was visually assessed for the remaining cases, and helmets that showed no conclusive evidence of damage were excluded. A purchasing phase then commenced for the remaining 37 helmets to collect identical samples for reconstruction. Many of the models, which were manufactured as early as 2004, were no longer in production by the manufacturer. Helmet models for which less than three samples could be obtained were excluded from the study. A total of 18 cases were designated as final reconstruction candidates.

#### *Damage Quantification*

For all candidate helmets, the nature and length of scrapes evident on the shell were recorded (the latter measured using digital calipers), and any damage related to the retention systems was noted. Each damaged helmet and an undamaged sample counterpart were then CT scanned (Aquilion, Canon Medical Systems, Tustin, CA: 120 kV, 200 mA,  $0.625 \times 0.625$  mm pixel spacing, 0.5 mm slice thickness). Scans were imported into Mimics Research 21.0 (Materialise, Leuven, Belgium), wherein helmet liners were separated from their shell and the surrounding environment using a Hounsfield Unit (HU) range of  $-960$  to  $-850$  followed by semi-automated segmentation operations. Final liner masks were converted into 3D surface mesh models comprised of  $>600,000$  triangular elements.

Liner models were imported into 3-matic Research 13.0 (Materialise, Leuven, Belgium) for damage quantification. An origin was defined at the base of the undamaged model at the center of its length and width. Damaged models were aligned with their undamaged counterpart using automated linear registration to minimize distances between a subset of similar nodes on each model. A global registration error was output from this process. A heat map reflecting approximate Hausdorff distances between each node on the undamaged model to the nearest node on the damaged

model was generated (Fig. 1). Heat map bounds were then set based on the global registration error in order to visualize the crush region in its entirety while minimizing noise.

The surface area exceeding the heat map bounds was recorded as the crush area. Bounds were then increased until a single node of the damaged liner was identified as being furthest offset from the undamaged liner. The radial thicknesses of the damaged and undamaged liners through this point were subtracted to yield max crush depth, and the corresponding point on the undamaged liner outer surface was recorded as the max crush location. The distance from this point to the crush area boundaries along the direction of helmet shell scraping was measured, and the ratio of superior/inferior or anterior/posterior measurements was computed to indicate the centeredness of the crush profile. Finally, a cylinder was defined that encompassed the crush area and extended radially through both models (Fig. 1). The volumes of the two models within this cylindrical region were subtracted to yield crush volume.

#### *Impact Testing*

Impact testing of the undamaged samples of each helmet was carried out using a custom, oblique impact rig.<sup>3</sup> Oblique impacts were generated through guided drop tests of a helmeted headform onto an adjustable-angled anvil (30–90 degrees from vertical in increments of 5 degrees), creating normal and tangential incident velocities characteristic of cyclist head impacts (Fig. 2). National Operating Committee on Standards for Athletic Equipment (NOCSAE) headforms in small (53.4 cm circumference), medium (57.6 cm), and large (61.4 cm) were used to account for the range in helmet sizes. NOCSAE headforms are common in sports helmet testing and have enhanced biofidelity compared to other headforms.<sup>10</sup> Helmets were fitted to the headforms according to manufacturer fit recommendations, then the helmeted headform was positioned in a support ring connected to the drop tower. The exact positioning of the headform for each test was measured using a dual-axis inclinometer (DMI600, Omni Instruments, Dundee, UK). Once set, the headform was secured in place using an additional support arm that released just prior to impact.

Initial impact velocity was recorded by a photogate for each test (BeeSpi V, NaRiKa Corp., Tokyo, Japan). Impact kinematics of the headform were collected at 20 kHz using three linear accelerometers (Endevco 7264B-2000, Meggitt Sensing Systems, Irvine, CA) and a tri-axis angular rate sensor (ARS3 PRO-18K, DTS, Seal Beach, CA) at the headform center of gravity (CG). Linear accelerations were



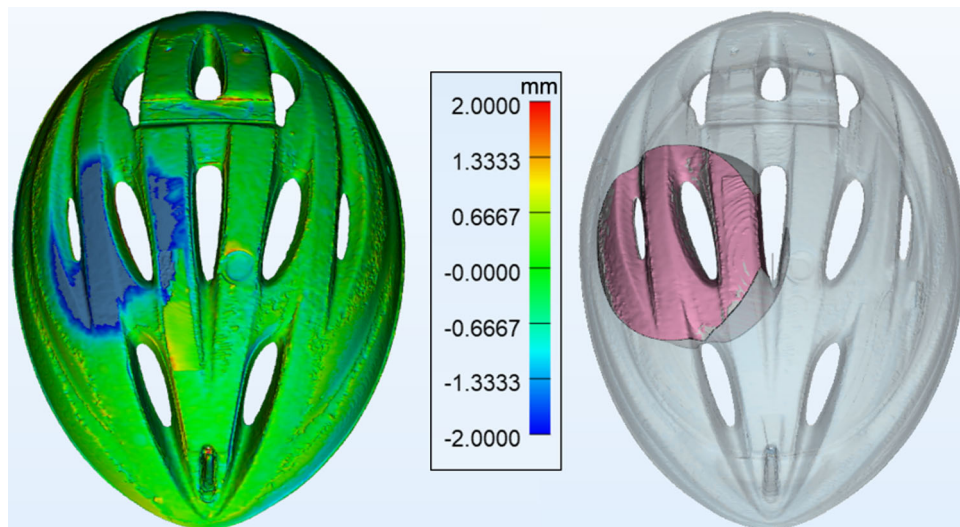


**FIGURE 1.** Damage quantification process for an exemplar helmet case. The area of crush exceeding  $-2.0$  mm is shown for illustration, with the cylindrical crush volume shown on the right.

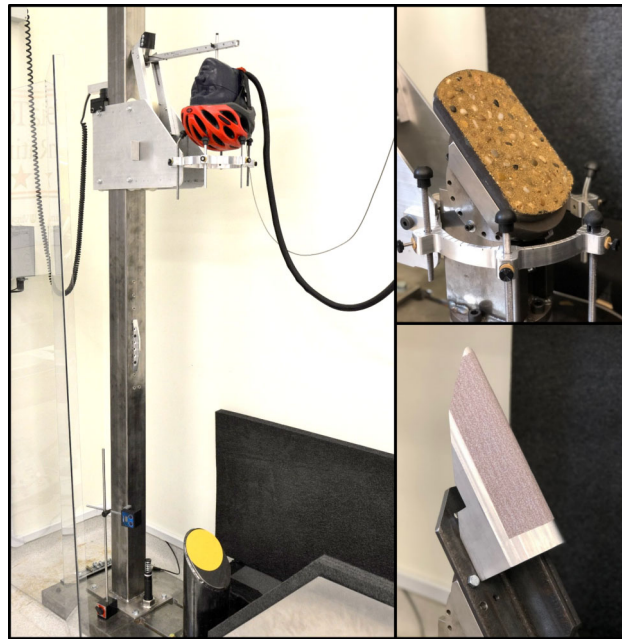


**FIGURE 2.** Oblique impact drop tower used for reconstruction testing. A variety of impact surfaces were employed to simulate different accident conditions. A sandpaper-coated steel anvil simulates a smooth road condition (left), while a rough anvil simulates a pockmarked road or sidewalk (top right), and a curbstone anvil provides a focal impact surface (bottom right).

processed using a channel frequency class (CFC) 1000 filter (SAE J211), while rotational velocities were processed using a CFC of 175.<sup>2</sup> Resultant curves were then computed and used to determine the PLA and peak rotational velocity (PRV) associated with each test. Although peak rotational acceleration (PRA) has historically also been investigated for its role in producing concussive injury, PRV has recently been suggested to be a superior correlate to brain tissue strain leading to concussion.<sup>18,20</sup> Further, analysis of the

PRA results (computed *via* differentiation of rotational velocity data) revealed strong correlations with PRV results for most cases herein, reflecting other helmeted head impact studies.<sup>29</sup> As such, only PRV results are reported.

An iterative process was employed for impact testing, in which each test's boundary conditions were updated based on visual assessment of damage from the previous test. A new, undamaged helmet was used per test. The orientation of the helmeted headform and

the angle of the anvil were set to replicate the direction of surface scraping and the max crush location for each helmet. It was generally assumed that all impacts were body driven (i.e. the head led the body in the direction of travel) unless the accident description hinted otherwise. The anvil surface was selected to best reflect the helmet's surface damage and the patient's description of the riding surface (Fig. 2); a steel surface coated with 80-grit sandpaper was used to simulate smooth road;<sup>14</sup> a "rough" surface comprised of a mixture of pebbles and sand in epoxy was used to simulate a pockmarked/bumpy road; and a curbstone was used to simulate more focal impact surfaces. Boundary conditions were updated between tests by adjusting the headform positioning, increasing or decreasing the anvil angle to alter the scrape length or visible crush area, and increasing or decreasing the drop height to alter the crush depth or crush area.

Prior to CT scanning the tested helmets, as many as three tests were conducted per case using a new, undamaged helmet per test. The overall goal of testing was to generate damage both more and less severe than the original helmet damage so that original impact conditions could be interpolated using linear models informed by damage metrics. CT scans were taken of the tested helmets and damage was quantified using the same approach used to quantify the original helmet damage. Damage metrics, including crush area, max crush depth, max crush depth location, crush centeredness, crush volume, and scrape length, were recorded and compared to the original damage. If any test produced a max crush location that was further from the original helmet max crush location than half the radius of the original helmet crush area, it was excluded from the analysis. Additional tests with updated boundary conditions were conducted as needed, with as many as seven tests in total conducted per case.

#### *Model Development and Statistics*

In order to generate estimates of the original impact conditions and head kinematics, multiple linear regression (MLR) models were developed for each case to relate damage metrics to impact conditions and kinematics. After testing was completed for a given case, damage metric results (scrape length, crush area, max crush depth, crush centeredness, and crush volume) from the tested helmets were first individually correlated with test normal and tangential velocities and PLA and PRV using Pearson's correlation coefficients. Damage metrics were correlated to normal and tangential velocities rather than impact angle and resultant velocity, as the relationships between damage and normal and tangential velocities are generally stronger and thought to be more mechanistic in nature.<sup>23</sup>

The two damage metrics that produced the most significant correlations with normal velocity were selected for input into the normal velocity MLR model, unless either was deemed likely to be associated with high error for that particular case (e.g. crush area measurement obscured by a nearby vent). The two damage metrics and their interaction were input as model terms given that there were enough trials to inform such a model; otherwise, models were built based on various combinations of the damage metrics, and the model with the greatest overall significance was determined. Least-significant terms were iteratively removed from the model until all remaining terms were significant or a model based on only one term and an intercept remained.

This process was repeated to determine an MLR model between tangential velocity and damage metrics, as well as between PLA and PRV and damage metrics. Resulting models were then solved using the damage metric values associated with the original helmet to generate estimates of the accompanying normal and tangential velocities and PLA and PRV for each case. The standard errors (SE) of each model at these estimates were determined. Associated impact resultant velocities and angles were then computed, with normal and tangential velocity standard errors propagated through in quadrature.

## RESULTS

The 18 cases included in the present study were associated with a range of accident characteristics, damage metrics, and injuries (Table 1). Following upper extremities, the head was the most commonly injured body region. Helmet damage locations corresponded with locations of superficial head injuries (when specified). Concussion was the most common non-superficial head injury diagnosis (7 out of the 18 cases), with loss of consciousness involved in four cases. Neck injuries were diagnosed in two cases, neither of which involved a concussion. Three cases involved helmets containing technology intended to reduce rotational kinematics of the head. One such case was associated with a concussion diagnosis. Helmet damage quantification revealed that the locations of max crush for both concussed and non-concussed patients were relatively interspersed (Fig. 3), suggesting that the two groups experienced impacts of similar directionality.

A majority of impacts were to the front and sides of the helmets, with very few to the top and rear regions (Table 1, Fig. 3). Five cases showed max crush locations very close to the helmet rim, and others showed evidence of surface scraping that extended down to the

**TABLE 1. Characteristics of each reconstruction case (Note: under the current AIS version, each concussion herein would have a severity score of 2; LOC loss of consciousness, SAH subarachnoid hemorrhage).**

Case	Helmet Style/Features	Head/Neck Injuries (AIS Severity)	Collision with	Riding surface	Damage location	Scrape length (cm)	Crush depth (mm)	Crush area (cm <sup>2</sup> )	Crush cent.	Crush vol. (cm <sup>3</sup> )
1	Multi-sport	Facial abrasion (1)	N/A	Pavement, holes/bumps	Frontal/temporal rim left	4.8	5.8	38.0	1.3	17.1
2	Road	Neck strain (1)	Moving vehicle	Pavement, debris	Parietal top	0.0	5.3	26.9	N/A	5.3
3	Urban	None	N/A	Pavement, holes/bumps	Temporal/parietal left	3.3	4.6	40.7	1.3	5.5
4	Multi-sport	None	Moving vehicle	Pavement, smooth	Parietal left	0.0	13.9	7.9	N/A	6.4
5	Road	None	N/A	Pavers	Frontal/temporal rim left	2.0	1.3	4.7	0.7	- 0.1 <sup>a</sup>
6	Road + Rot. tech	Facial laceration (1)	Cyclist	Pavement, smooth	Frontal/temporal rim left	2.7	0.3	0.0	0.2	0.0
7	Road + Rot. tech	None	N/A	Concrete, holes/bumps	temporal rim left	6.0	3.2	15.4	1.2	3.9
8	Multi-sport	Concussion with LOC (2) Left forehead abrasion (1)	N/A	Pavement, smooth	occipital left	6.0	3.2	20.4	0.5	1.1
9	Multi-sport	Concussion, no LOC (1) Left eye abrasion (1)	Moving vehicle	Pavement, holes/bumps	parietal left	0.0	5.7	34.9	N/A	16.0
10	Road	Left maxillary abrasion (1)	Moving vehicle	Pavement, smooth	Parietal rear top/left	11.0	3.4	46.1	0.5	16.8
11	Multi-sport	Concussion, no LOC (1)	Patient unsure	Patient unsure	Frontal/parietal left	3.2	4.4	17.3	6.2	2.6
12	Urban	Right forehead abrasion (1) Right parietal scalp contusion (1) C6 lamina fracture (2)	Parked vehicle	Pavement, smooth	Temporal rim right Frontal right	11.0	6.1	88.4	0.2	29.4
13	Road	Right frontal SAH with LOC (2) Concussion with LOC (2)	N/A	Pavement, holes/bumps	Temporal/parietal left	8.0	9.7	56.5	0.4	18.1
14	Multi-sport	Concussion with LOC (2)	N/A	Train tracks	Frontal center/right	13.0	2.7	6.4	3.4	0.6
15	Urban	Concussion with LOC (2)	Motorcycle/ scooter	Pavement smooth	Parietal/occipital left	0.6	2.3	18.1	1.2	11.3
16	Road + Rot. tech	Concussion, no LOC (1)	N/A	Pavement, holes/bumps	Frontal/temporal right	2.0	4.6	22.3	3.3	7.6
17	Road	Left temple abrasion (1)	Moving vehicle	Pavement, smooth	Temporal/parietal left	11.0	4.1	40.2	6.1	9.1
18	Road	Right and central facial abrasions (1)	Cyclist	Pavement, smooth	Temporal/parietal right	7.0	4.9	24.3	0.3	6.9

<sup>a</sup>The minimal damage to this helmet produced a crush volume that likely fell within the noise floor of the CT scans and manufacturing variability; volume is essentially 0.

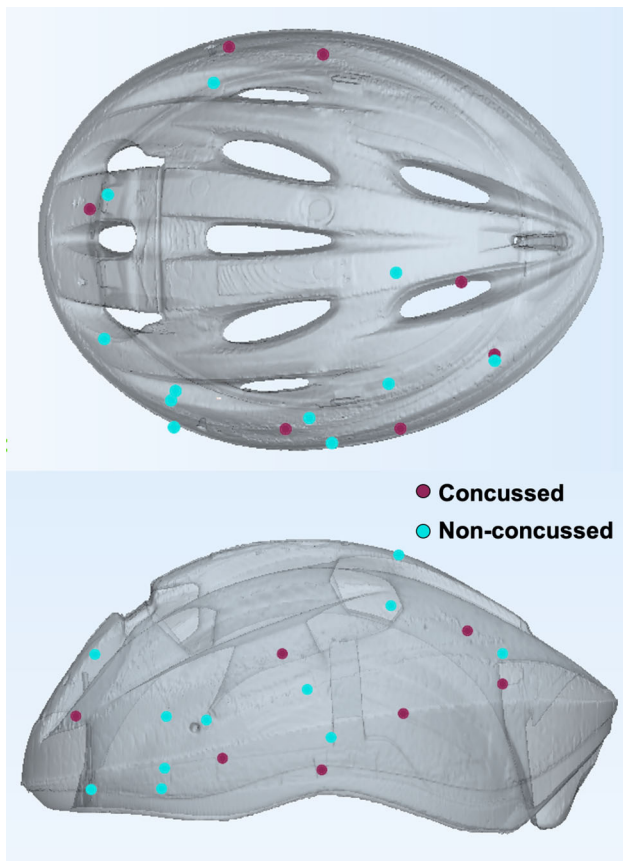


**FIGURE 3.** Locations of max crush for all cases, modeled on an exemplar helmet and grouped by concussive injury diagnosis. A majority of impacts were to the front and sides of the helmets, often near the helmet rim.

rim despite superior max crush locations. The average scrape length across all original helmets was  $5.7 \pm 4.1$  cm. Max crush depth ranged from 0.3 to 13.9 mm across all cases, while crush area ranged from 0 to 88.4 cm<sup>2</sup>, centeredness ranged from 0.2 to 6.2, and volume ranged from  $-0.1$  to 29.4 cm<sup>3</sup> (the negative lower bound reflects minimal damage for one case combined with inherent noise from manufacturing differences and CT processing). Damage related to retention systems was noted in a few cases and could be recreated to an extent through impact testing.

A variety of test conditions were required to simulate the damage associated with each case. A summary of the test conditions and results is provided in the Appendix. The smooth road anvil was used for the majority of cases. Three helmets did not appear to be scraped while still presenting with liner damage. Normal impacts were conducted for these cases. Several cases indicated that the impact was caused by collision with a vehicle; however, the description did not specify what surface the helmet came in contact with. The decision of which anvil to use for these cases was thus

informed primarily by assessment of surface damage, with the curbstone anvil selected for two cases.

Data from an average of four tests were included in the MLR models for each case. In order to interpolate velocity and kinematic estimates rather than extrapolate, some cases required more tests than others if initial testing produced damage that was consistently too severe or not severe enough relative to the original helmet damage. Matching impact locations during testing was often more difficult when steeper anvil angles were involved, as the headform's rotation was challenging to predict and varied with its initial orientation. For cases 5 and 7, data from only two tests could be included in the MLR models. Estimates for these cases were interpolated, and error was reported as the range between the solution and the further of the two test values. Case 4 was associated with a unique damage pattern, in which liner peaks at the rear of the helmet were avulsed but the surrounding liner was minimally damaged. Normal-velocity curbstone impacts were conducted for this case. It was observed that the liner peaks avulsed from the helmet once the normal velocity reached a particular severity. Impact conditions and kinematics from the lowest-velocity test producing this avulsion were assigned as the estimates for this case, while error was determined using the difference between these results and the results of the nearest lower velocity test. All other cases showed more typical damage profiles that could be characterized by a number of damage metrics.

A typical helmet-specific MLR model is shown in Eq. 1 (case 14). This normal velocity (*Norm*) model reflects that max crush depth (*Depth*) and crush area (*Area*) were the most significant predictors of normal velocity for this helmet ( $p = 0.01$  for *Depth* vs. *Norm*,  $p = 0.09$  for *Area* vs. *Norm*). Max crush depth and area, along with the interaction term, were thus input into the MLR model. Removing the least significant term produced Eq. (1)—a finalized MLR model wherein all term coefficients and the overall model were significant ( $p < 0.02$ ).

$$Norm = 0.78 + 0.56Depth - 0.01Depth * Area \quad (1)$$

Across all cases, the normal velocity MLR models were most frequently informed by max crush depth. Tangential velocity models were most frequently informed by crush volume, PLA models were most frequently informed by crush area and depth, and PRV models were informed most frequently by crush area (followed closely by scrape length and crush volume). Tangential velocity and PRV models were sometimes informed by crush centeredness, although crush centeredness was the least common predictor across all models. Average standard errors associated with normal and tangential velocity estimates were 0.15 and 0.22 m/s, respectively, while average standard errors



associated with PLA and PRV were 5.4 g and 1.4 rad/s. The median normal velocity across all cases was 3.4 m/s with a 95% range of 0.24 m/s and 6.0 m/s (2.5th and 97.5th percentiles, respectively; Fig. 4). The median tangential velocity was 3.8 m/s (95% range:  $-0.02$ , 7.5 m/s). The negative lower bound was influenced by a single case with a tangential velocity estimate of  $-0.04$  m/s. This particular helmet had minimal damage, meaning the results were subject to greater noise ratios. The estimated impact angles reflected anvil angles used in testing, with a median of  $40.3^\circ$  across all cases (95% range:  $26.3^\circ$ ,  $90^\circ$ ). The median estimated resultant velocity was 5.5 m/s (95% range: 0.4 m/s, 8.5 m/s). Average errors associated with impact angle and resultant velocity were  $0.3^\circ$  and 0.2 m/s.

Estimated head impact PLA ranged from 11.1 to 218.8 g across all cases with a median of 102.5 g. PRV ranged from 2.1 to 48.1 rad/s with a median of 22.3 rad/s. PLA and PRV generally increased with increasing normal and tangential velocities, respectively. The correlation between PLA and normal velocity was significant ( $R = 0.61$ ,  $p = 0.01$ ), while the correlation between PRV and tangential velocity was not ( $R = 0.35$ ,  $p = 0.16$ ). The single case associated

with subarachnoid hemorrhage produced the greatest PLA of 218.8 g. Kinematic results were not significantly different between concussed and non-concussed groups ( $p \geq 0.37$ ). Cases associated with a concussion produced an average PLA and PRV of  $109.8 \pm 55.0$  g and  $19.3 \pm 7.4$  rad/s, respectively, compared to averages of  $98.1 \pm 58.5$  g and  $24.2 \pm 14.8$  rad/s for non-concussion cases (Fig. 5).

## DISCUSSION

The goal of the present study was to use oblique impacts and CT to investigate common cyclist head impact conditions and kinematics. Across all donated helmets, maximum crush locations most often fell at the front and sides of the helmets, frequently near the rim. These locations are consistent with previously reported cyclist head impact locations.<sup>7,32,34</sup> Impacts to the helmet rim are of particular importance, as helmet safety standards exclude the helmet rim during impact testing, meaning its impact performance is not regulated. Specifically, five of the cases herein fell at or below the CPSC test line. The present results supple-

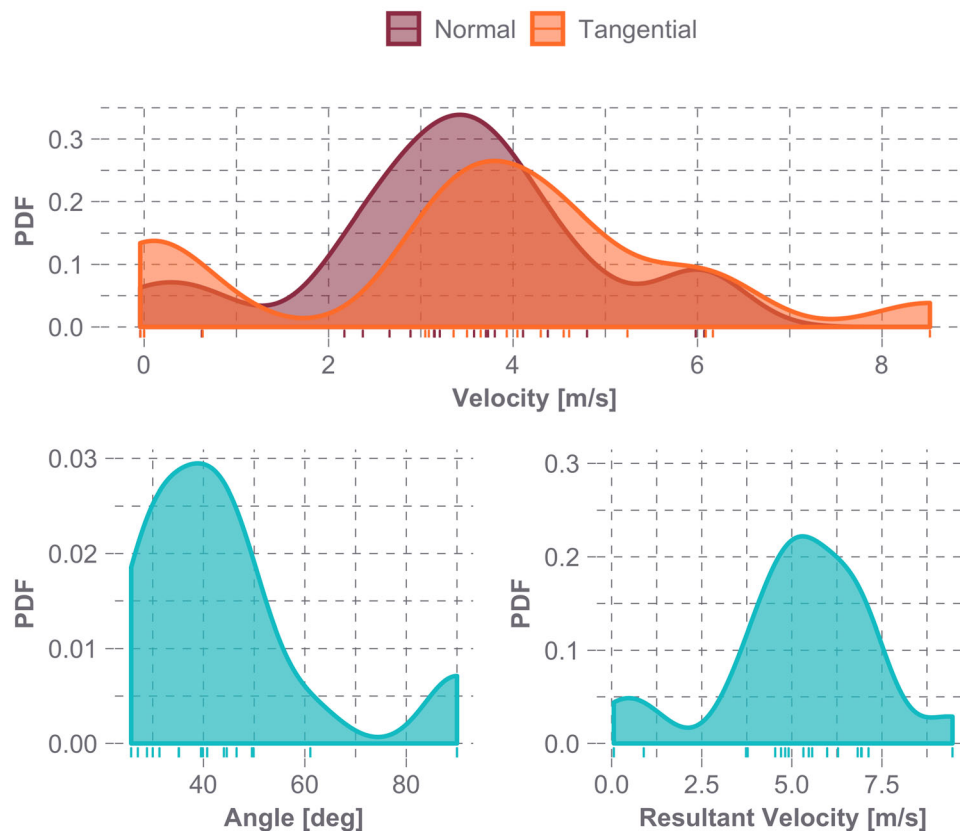


**FIGURE 4.** Probability density functions (PDFs) of all normal and tangential velocity estimates and associated impact angle and resultant velocity estimates. The impact angle is the angle between the resultant velocity vector and the impact surface, such that 90 degrees represents a purely normal impact. The vertical lines underneath each plot are the individual data points that make up the distribution.



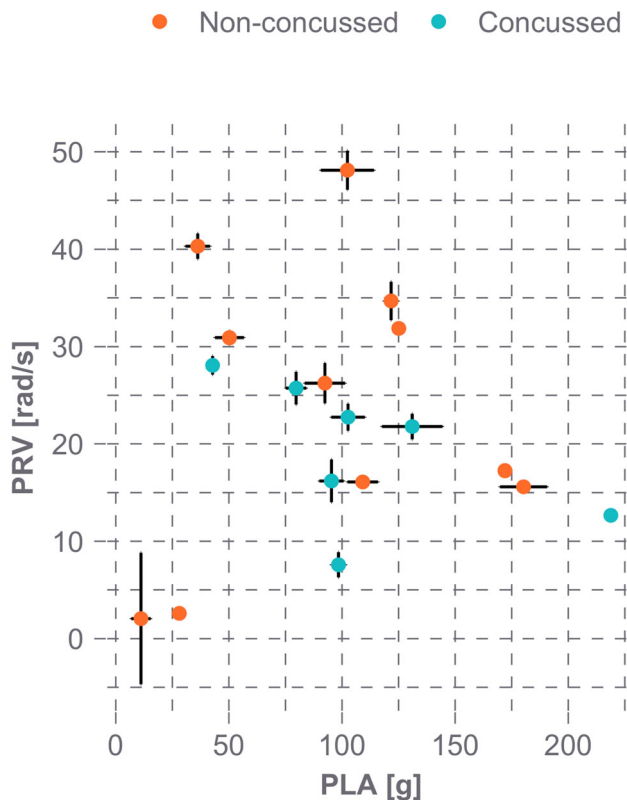


**FIGURE 5. PLA and PRV estimates for each case and the associated concussive injury diagnosis. Concussive and non-concussive kinematics were interspersed, with average PLA and PRV not differing significantly across groups.**

ment a growing body of evidence suggesting that the rim is a commonly impacted helmet region. Although not evident in these results, high-energy impact tests have previously demonstrated liner densification at the rim for some certified helmets, which in turn transfers very large and likely injurious forces to the head.<sup>4,13</sup> DeMarco et al. subjected helmets to CPSC testing and found that many allowed PLA values above the 300 g threshold when tested at the rim (and sometimes above the rim), even though the helmet were reportedly CPSC-certified.<sup>13</sup> It is therefore recommended that standards be adapted so that helmet protective capabilities are regulated at the rim.

The median normal velocity and PLA found in the present study fell considerably below the test velocities and PLA thresholds defined in standards. The CPSC standard requires normal impacts against a flat anvil at 6.2 m/s and imposes a PLA limit of 300 g.<sup>12</sup> Only two of the 18 cases herein were associated with normal velocities greater than or equal to 6 m/s, and none were associated with a PLA greater than 219 g. While it is essential for standards to ensure risk of catastrophic injury is mitigated, the present results suggest that less severe impacts are common in cyclist crashes and have the potential to produce concussion. Additionally, a

majority of impacts herein were oblique, involving substantial tangential velocities and producing considerable PRVs. As rotational kinematics have been tied to concussive injury mechanisms,<sup>16,18–20</sup> there would be value in standards assessing the ability of helmets to reduce both linear and rotational head kinematics during oblique impacts.

The velocity and kinematic estimates generated herein were similar to ranges reported from previous cyclist simulation and damage reconstruction studies.<sup>7,27,32,34</sup> The median normal velocity and PLA in the present study were near matches to median values from other reconstruction studies that employed normal impacts using standards test equipment.<sup>32,34</sup> Previous work has demonstrated that liner crush depth is strongly correlated with impact normal velocity, which in turn is well-correlated with PLA.<sup>5,24</sup> Given that the NOCSAE headform mass is comparable to the headform mass in standards, it is intuitive that normal velocity and PLA results might be comparable across studies. These similarities suggest that the present results reflect common cyclist head impact conditions. Utilization of oblique impact testing to quantify damage has the added benefit of estimating associated tangential velocities and PRV as well, which has meaningful implications for injury risk assessment. Compiling published cyclist simulation data reveals slightly greater median head impact velocities and slightly lower angles than this study found,<sup>7,27</sup> although overall distributions are markedly similar.

MLR models relating damage metrics to impact conditions and kinematics for each case revealed that normal velocity and PLA models were commonly informed by max crush depth, tangential velocity was commonly informed by crush volume, and PRV was commonly informed by crush area and scrape length. However, there were often deviations from these trends. It is likely that the relationships between damage metrics and impact velocities or kinematics are modulated by the specific helmet model as well as the impact location. For example, proximity of a vent to the impact location can obfuscate measurement of scrape length or crush area. There is therefore benefit to creating individualized models to predict impact conditions on a case-specific basis.

Grouping kinematic results by concussion diagnosis revealed surprising trends, or rather a lack thereof. The high number of concussions in this dataset supports epidemiological evidence of concussion being a common injury for cyclists.<sup>11</sup> However, risk of concussion is known to increase with increasing impact kinematics,<sup>28</sup> and rotational kinematics in particular have been implicated as a causative factor in concussion.<sup>16,18–20</sup> In the present study, PLA and PRV were not significantly different across concussed and non-concussed

cases. The average PLA of the concussed group was consistent with median concussive PLAs reported in football head impact datasets,<sup>28</sup> while the average PRV of the concussed group was somewhat lower than median concussive PRVs (Rowson *et al.*: 21.9 rad/s).<sup>29</sup> Although there is considerable subject-to-subject variation in susceptibility to concussion,<sup>28</sup> it is also possible that differences in injury reporting across cases contributed to this trend. In the present dataset, all cases with a diagnosed concussion stemmed from one hospital. This likely relates to the fact that concussion is characterized by physiological symptoms rather than anatomical damage, meaning that its diagnosis can be more subjective and less standardized across different institutions than other injuries. Inherent error in the reconstruction process may have also contributed to the lack of trends observed. Regardless, the high incidence of concussion out of these cases suggest there is room for improvement in helmet design to reduce risk of concussion.

The lack of significant differences in kinematics across concussed versus non-concussed groups may also reflect the general nature of damage reconstruction studies. Reconstructing damage to a helmet requires that the helmet present with a definitive damage region. Permanent EPS crush requires that the foam be subject to stresses exceeding its yield stress. It is possible that some cyclists impacted their head at too low of a severity to induce substantial damage. Supporting this theory, several non-concussed patients claimed that their helmet was damaged during their crash, while visual assessment and CT scans of the helmet did not identify a definitive damage region. If a head impact did occur, it is likely that the associated kinematics were extremely low. Excluding such cases from reconstruction likely over-weights resulting non-concussive kinematics and blurs the distinction between concussed and non-concussed groups. Additionally, the overarching IIHS study through which cyclists were recruited required them to remember the route they were biking on at the time of their crash;<sup>9</sup> the 44 patients who did not meet this requirement may have comprised a number of the possible concussion cases.

There are a number of limitations associated with the present study. Similar to previous oblique impact studies, no surrogate neck was used in impact testing.<sup>3,24,25</sup> This decision was motivated by the limited biofidelity of the commonly-used Hybrid III neck in compressive axial loading,<sup>30</sup> which may have been present in large amounts for cases with damage near the top of the helmet and impact angles near 90°. However, previous studies have suggested that the contraction of neck musculature may affect head impact kinematics to a limited extent,<sup>15</sup> and others have shown that oblique impacts involving a neck or body mass could result in decreased head kinematics and increased liner crush depth compared to head-only

impacts.<sup>2,17</sup> Additionally, the headform used herein may produce slight differences in helmet damage compared to a human head.<sup>5</sup> The anvils used also likely produced marginally more severe results than a road due to exaggerated stiffness and frictional properties.<sup>6</sup>

Assumptions had to be made during testing regarding the direction of impact and the impact surface. It was also assumed for all cases that the helmet was positioned correctly on the head prior to impact. A few cases possibly involved multiple head impacts. In such cases, the primary impact location was assumed to be at the max crush location. Two cases with extensive damage had longer scrape lengths than could be replicated using a single impact, even when max crush depth was matched and the steepest angle was employed. It is possible that extended, body-driven contact between the head and impact surface occurred in these cases, which would be of lesser force than the initial impact phase.

Other potential sources of error were evident during CT scan processing. Although helmet attachments were removed prior to scanning, the presence of cages or riveting caused patches of scan artifact for several cases. These fortunately did not often overlap with the crush region and were manually corrected. Damage metric quantification was also complicated at times by proximity to a vent. MLR models were developed with consideration given to these issues.

As the present helmets were provided from emergency departments in urban settings, these cases may reflect higher-severity accidents and may be specific to an urban environment. However, fatality cases were excluded, while a number of cases did not involve head injury at all, suggesting a wide range in head impact severities was represented. Additionally, the limited sample size involved in this study precluded assessment of the effectiveness of different style helmets or helmets with rotation-mitigating technologies.

Despite its limitations, this study represents one of the most advanced bicycle helmet damage reconstructions to-date. Damage to 18 bicycle helmets from real-world cyclist accidents was quantified using CT and recreated through oblique impacts. The similarities between results from this study and past studies, paired with the low associated errors, instills confidence in the overall results. The impact conditions and resulting kinematics determined in this work can help to inform realistic boundary conditions for oblique impact testing of bicycle helmets, equipping manufacturers to optimize helmet protective capabilities.

## APPENDIX

**TABLE A1. Testing and model results for each case. Standard errors (SE) are provided for normal and tangential velocities, PLA, and PRV, while the propagated errors from the normal and tangential velocity SE are given for resultant velocity and impact angle.**

Case	Test surface/headform size	Normal velocity (SE) (m/s)	Tangential velocity (SE) (m/s)	Resultant velocity (error) (m/s)	Impact angle(error) (°) (vertical)	PLA (SE) (g)	PRV (SE) (rad/s)
1	Smooth road <sup>a</sup> /Medium	3.1 (0.1)	6.2 (0.5)	6.9 (0.4)	27.1 (0.1)	109.1 (6.8)	16.1 (0.3)
2	Curbstone/Medium	3.7 (0.4)	0.0 (N/A)	3.7 (0.4)	90 (N/A)	92.4 (8.9)	26.2 (2.1)
3	Smooth road <sup>a</sup> /Medium	3.6 (0.1)	3.0 (0.2)	4.7 (0.1)	49.6 (0.1)	172.0 (0.4)	17.3 (0.5)
4	Curbstone/Medium	6.0 (0.5)	0.0 (N/A)	6.0 (0.5)	90 (N/A)	36.2 (5.4)	40.3 (1.3)
5	Smooth road/Large	0.6 (0.1)	0.6 (0.1)	0.9 (0.1)	44.6 (0.1)	28.1 (2.1)	2.6 (0.3)
6	Smooth road <sup>a</sup> /Medium	0.0 (0.1)	0.0 (0.1)	0.1 (0.1)	46.5 (1.4)	11.1 (4.3)	2.1 (6.8)
7	Curbstone/Small	2.7 (0.3)	4.6 (0.5)	5.3 (0.4)	30.0 (0.5)	50.2 (6.4)	30.9 (0.7)
8	Rough road <sup>a</sup> /Medium	2.4 (0.1)	4.3 (0.2)	4.9 (0.2)	28.9 (0.2)	95.3 (5.4)	16.2 (2.2)
9	Smooth road <sup>a</sup> /Medium	4.8 (0.3)	4.0 (0.3)	6.3 (0.3)	49.9 (0.6)	102.7 (7.4)	22.7 (1.4)
10	Smooth road <sup>a</sup> /Medium	3.7 (0.0)	6.1 (0.0)	7.1 (0.0)	31.3 (0.1)	102.4 (11.8)	48.1 (2.0)
11	Smooth road/Small	2.9 (0.0)	3.5 (0.1)	4.5 (0.1)	39.5 (0.1)	98.4 (3.2)	7.6 (1.3)
12	Smooth road <sup>a</sup> /Medium	4.1 (0.1)	8.5 (0.4)	9.5 (0.4)	25.7 (0.4)	121.7 (3.2)	34.7 (2.0)
13	Rough road/Medium	6.1 (0.0)	3.4 (0.5)	6.9 (0.2)	61.1 (0.0)	218.8 (0.2)	12.7 (0.1)
14	Curbstone/Medium	2.2 (0.0)	3.1 (0.1)	3.8 (0.1)	35.1 (0.0)	42.8 (0.9)	28.1 (1.3)
15	Smooth road/Small	3.1 (0.4)	3.6 (0.1)	4.8 (0.2)	40.7 (0.6)	131.0 (13.4)	21.8 (1.3)
16	Rough road/Medium	3.8 (0.2)	3.9 (0.3)	5.5 (0.3)	44.0 (0.5)	79.7 (4.6)	25.7 (1.7)
17	Smooth road <sup>a</sup> /Medium	3.2 (0.0)	4.5 (0.1)	5.6 (0.1)	35.2 (0.1)	125.1 (0.3)	31.9 (0.2)
18	Rough road <sup>a</sup> /Small	4.4 (0.1)	5.2 (0.4)	6.8 (0.3)	39.9 (0.2)	180.2 (10.4)	15.6 (0.4)

<sup>a</sup>The anvil surface did not match the patient's description of the riding surface, but was instead chosen to reflect the nature of damage to the exterior of the helmet. This was deemed suitable because it was not guaranteed that patients struck their head on the same surface on which they were riding and because not all patients remembered the exact riding surface.

## ACKNOWLEDGMENTS

The authors would like to thank the Insurance Institute for Highway Safety (IIHS) and the Virginia Tech Institute for Critical Technology and Applied Science (ICTAS) for their funding and support, the Virginia-Maryland College of Veterinary Medicine for CT scanner use, Materialise application engineers for aiding in the software-based analysis, Kamil Narayan for managing data collection at Oregon Health and Science University, and all research assistants who enrolled and interviewed patients for the study.

## CONFLICT OF INTEREST

The authors have no conflicts of interest to declare.

## REFERENCES

- <sup>1</sup>Association, Governors Highway Safety Association. A Right to the Road: Understanding and Addressing Bicyclist Safety, 2017.
- <sup>2</sup>Bland, M. L., C. McNally, and S. Rowson. Headform and neck effects on dynamic response in bicycle helmet oblique impact testing. In: *Proceedings of the IRCOBI Conference*, Athens, Greece, 2018, pp. 413–423.
- <sup>3</sup>Bland, M. L., C. McNally, *et al.* Development of the STAR evaluation system for assessing bicycle helmet protective performance. *Ann. Biomed. Eng.* 48:47–57, 2020.
- <sup>4</sup>Bland, M. L., D. S. Zuby, B. C. Mueller, and S. Rowson. Differences in the protective capabilities of bicycle helmets in real-world and standard-specified impact scenarios. *Traffic Inj. Prev.* 19(sup1):S158–S163, 2018.
- <sup>5</sup>Bonin, S. J., J. F. Luck, *et al.* Dynamic response and residual helmet liner crush using cadaver heads and standard headforms. *Ann. Biomed. Eng.* 45(3):656–667, 2017.
- <sup>6</sup>Bonugli, E. The effects of dynamic friction in oblique motorcycle helmet impacts. In: *Biomedical Engineering*. Ann Arbor: The University of Texas at San Antonio, 2015, p. 78.
- <sup>7</sup>Bourdet, N., C. Deck, *et al.* In-depth real-world bicycle accident reconstructions. *Int. J. Crashworthiness* 19(3):222–232, 2014.
- <sup>8</sup>Chinn, B., B. Canaple, *et al.* COST 327: Motorcycle Safety Helmets, edited by B. Chinn. Belgium: European Commission, Directorate General for Energy and Transport, 2001.
- <sup>9</sup>Ciccino, J. B., M. L. McCarthy, *et al.* Not all protected bike lanes are the same: infrastructure and risk of cyclist collisions and falls leading to emergency department visits in three U.S. cities. *Insurance Institute for Highway Safety*, July 2019.
- <sup>10</sup>Cobb, B. R., A. MacAlister, *et al.* Quantitative comparison of Hybrid III and National Operating Committee on Standards for Athletic Equipment headform shape characteristics and implications on football helmet fit. *Proc. IMechE P JSET* 229(1):39–46, 2014.
- <sup>11</sup>Coronado, V. G., T. Haileyesus, *et al.* Trends in sports- and recreation-related traumatic brain injuries treated in US Emergency Departments: The National Electronic Injury Surveillance System-All Injury Program (NEISS-AIP) 2001–2012. *J. Head Trauma Rehabil.* 30(3):185–197, 2015.
- <sup>12</sup>CPSC. Safety Standard for Bicycle Helmets Final Rule (16 CFR Part 1203), 1998.
- <sup>13</sup>DeMarco, A. L., D. D. Chimich, S. J. Bonin, *et al.* Impact performance of certified bicycle helmets below, on and above the test line. *Ann. Biomed. Eng.* 48:58–67, 2020.
- <sup>14</sup>ECE. R-22.05: Uniform provisions concerning the approval of protective helmets for drivers and passengers of motorcycles and mopeds, 1999.
- <sup>15</sup>Eckersley, C. P., R. W. Nightingale, J. F. Luck, and C. R. Bass. Effect of neck musculature on head kinematic response following blunt impact. *Proceedings of the IRCOBI Conference*. Antwerp, Belgium, 2017, pp. 685–698.
- <sup>16</sup>Gennarelli, T., A. Ommaya, and L. Thibault. Comparison of translational and rotational head motions in experimental cerebral concussion. *Proceedings of 15th Stapp Car Crash Conference*, 1971.
- <sup>17</sup>Ghajari, M., S. Peldschus, U. Galvanetto, and L. Iannucci. Effects of the presence of the body in helmet oblique impacts. *Acc. Anal. Prev.* 50:263–271, 2013.
- <sup>18</sup>Hardy, W. N., M. J. Mason, *et al.* A study of the response of the human cadaver head to impact. *Stapp Car Crash J.* 51:17–80, 2007.
- <sup>19</sup>King, A. I., K. H. Yang, *et al.* Is head injury caused by linear or angular acceleration? *IRCOBI Conference*, 2003. Lisbon, Portugal. pp. 1–12.
- <sup>20</sup>Kleiven, S. Predictors for traumatic brain injuries evaluated through accident reconstructions. *Stapp Car Crash J.* 51:81–114, 2007.
- <sup>21</sup>Loftis, K. L., D. P. Moreno, *et al.* Utilizing computed tomography scans for analysis of motorcycle helmets in real-world crashes. *Proceedings of 48th RMBS Conference*, 2011. Denver, Colorado.
- <sup>22</sup>Mertz, H. J., A. L. Irwin, and P. Prasad. Biomechanical and scaling bases for frontal and side impact injury assessment reference values. *Stapp Car Crash J.* 47:155–188, 2003.
- <sup>23</sup>Mills, N. J. Critical evaluation of the SHARP motorcycle helmet rating. *Int. J. Crashworthiness* 15(3):331–342, 2010.
- <sup>24</sup>Mills, N. J., and A. Gilchrist. Oblique impact testing of bicycle helmets. *Int. J. Impact Eng.* 35(9):1075–1086, 2008.
- <sup>25</sup>Milne, G., C. Deck, *et al.* Bicycle helmet modelling and validation under linear and tangential impacts. *Int. J. Crashworthiness* 19:323–333, 2014.
- <sup>26</sup>Olivier, J., and I. Radun. Bicycle helmet effectiveness is not overstated. *TIP* 18(7):755–760, 2017.
- <sup>27</sup>Peng, Y., Y. Chen, *et al.* A study of pedestrian and bicyclist exposure to head injury in passenger car collisions based on accident data and simulations. *Saf. Sci.* 50(9):1749–1759, 2012.
- <sup>28</sup>Rowson, S., and S. M. Duma. Brain injury prediction: assessing the combined probability of concussion using linear and rotational head acceleration. *Ann. Biomed. Eng.* 41(5):873–882, 2013.
- <sup>29</sup>Rowson, S., S. M. Duma, *et al.* Rotational head kinematics in football impacts: an injury risk function for concussion. *Ann. Biomed. Eng.* 40:1–13, 2012.
- <sup>30</sup>Sances, A. J., F. Carlin, and S. Kumaresan. Biomechanical analysis of headneck force in Hybrid III dummy during inverted vertical drops. *Biomed. Sci. Instrum.* 38:459–464, 2002.
- <sup>31</sup>Sanford, T., C. E. McCulloch, and R. A. Callcut. Bicycle trauma injuries and hospital admissions in the United States, 1998–2013. *JAMA* 314(9):947–949, 2015.



- <sup>32</sup>Smith, T. A., D. Tees, D. R. Thom, and H. H. Hurt. Evaluation and replication of impact damage to bicycle helmets. *Accid. Anal. Prev.* 26(6):795–802, 1994.
- <sup>33</sup>Thompson, D. C., F. P. Rivara, and R. S. Thompson. Effectiveness of bicycle safety helmets in preventing head injuries. A case-control study. *JAMA* 276(24):1968–1973, 1996.

- <sup>34</sup>Williams, M. The protective performance of bicyclists' helmets in accidents. *Accid. Anal. Prev.* 23(2–3):119, 1991.

**Publisher's Note** Springer Nature remains neutral with regard to jurisdictional claims in published maps and institutional affiliations.